THE ASTROPHYSICAL JOURNAL, 409:179–189, 1993 May 20

MODELS FOR THE MAGNETIC FIELD OF M81

DAVID MOSS
Mathematics Department, The University, Manchester M13 9PL, UK
AXEL BRANDENBURG
NORDITA, Blegdamsvej 17, DK-2100 Copenhagen Ø, Denmark
KARL JOHAN DONNER
Observatory and Astrophysics Laboratory, University of Helsinki, Tähtitorninmäki, SF-00130 Helsinki, Finland
AND
MAGNUS THOMASSON
NORDITA, Blegdamsvej 17, DK-2100 Copenhagen Ø, Denmark
Received 1992 July 29; accepted 1992 October 27

ABSTRACT

We study several mean field dynamo models in disk geometry in an attempt to understand the origin of the nonaxisymmetric magnetic field present in M81. There appear to be three (at least) relevant mechanisms, which are not mutually exclusive. Because field growth times are not very short compared to galactic ages, a predominantly nonaxisymmetric seed field may still give a significantly nonaxisymmetric field after times of order 10^{10} yr, even if the stable field configuration is axisymmetric. The spiral structure may give a nonaxisymmetric structure to the disk turbulence, and thus to the turbulent coefficients appearing in mean field dynamo theory. Third, M81 may have undergone a close encounter with a companion galaxy. A dynamical model of the interaction predicts strong, nonaxisymmetric, large-scale gas velocities in the disk plane, and these can produce nonaxisymmetric fields. In the absence of the second of these effects, our models predict that nonaxisymmetric fields will be present in the outer parts of the galaxy, together with significant axisymmetric contributions in the inner part. However, we do not find that any of these effects, taken individually, can produce dominant nonaxisymmetric field structure. If they are simultaneously present, they can reinforce one another. Further, our calculations are for a relatively thick disk (thickness to radius ratio of order 0.2), and a reduction to smaller, and plausibly more realistic, values will also favor nonaxisymmetric field generation.

Subject headings: galaxies: individual (M81) — magnetic fields — ISM: magnetic fields — MHD

1. INTRODUCTION

Observations suggest the presence of a significant nonaxisymmetric component of magnetic field in the spiral galaxy M81, although the evidence for such fields (bisymmetric spirals hereafter BSS) in other galaxies has been controversial during the last few years (cf. the various opinions expressed in Sofue, Fujimoto, & Wielebinski 1986 and Beck 1990). Investigations of mean field dynamos in thin disks do not find nonaxisymmetric fields to be more easily excited than axisymmetric unless, for example, large anisotropies are invoked in the alpha-coefficient (e.g., Meinel, Elstner, & Rüdiger 1990; Elstner, Meinel, & Beck 1992), although the critical dynamo numbers may become approximately equal as the ratio of disk height to radius becomes small (Ruzmaikin, Shukurov, & Sokoloff 1988; Moss & Brandenburg 1992). On the other hand, the relative sizes of the critical dynamo numbers may not be the relevant criterion even in the weakly nonlinear regime (e.g., Brandenburg et al. 1989). Moreover, unlike stellar dynamos, growth times of magnetic fields in galaxies are not very short compared to the lifetime of the embedding system (ca. a Hubble time) and galactic dynamos may not have existed long enough for all transient behavior to have disappeared (e.g., Moss & Tuominen 1990). Studies of the Faraday rotation measures have not yet revealed any evidence of cosmological evolution (Perry, Watson, & Kronberg 1992). Brandenburg et al. (1992, hereafter Paper I) investigated the excitation of strictly axisymmetric modes in a two-component galaxy model, where the resistivity in the halo exceeds that in the disk, and the alpha effect may be more-or-less concentrated to the disk. They find the evolution of the field to be quite complicated, because of the different growth rates in the disk and halo regions, and the differing stability of fields with odd and even parity with respect to the galactic plane. In particular, the fastest growing modes may not be of the same parity type as the eventually stable modes found after nonlinear effects have had time to act. For example, an even parity (S0) field located in the disk may initially be present, but be unstable to the presence of an odd parity (A0) halo mode, which grows more slowly but eventually dominates. Evolutionary times are long enough that these transient effects could be important when trying to account for the field geometries deduced from observations of rotation measures.

In this paper we study the evolution of seed fields containing both nonaxisymmetric and axisymmetric parts, in a galactic model with distinct disk and halo components. The halo is assumed to be spherical and embedded in a vacuum, which simplifies the imposition of the boundary conditions. This approach was introduced by Stepinski & Levy (1988), and in cylindrical geometry by Elstner, Meinel, & Rüdiger (1990) and was also used in Moss & Tuominen (1990). The initial field energy is assumed to be substantially less than the equipartition value, and we introduce nonlinearity by a simple α-quenching mechanism. We find that with a seed field that is

dominated by a $m = 1$ component (assuming azimuthal dependence $e^{im\phi}$), significant $m = 1$ structure can persist for times of order 10^{10} yr.

We also discuss other mechanisms that may encourage the persistence of $m = 1$ structure. M81 is a member of a small group of galaxies. Recently, Thomasson & Donner (1992) have presented a model in which the spiral structure of M81 is generated in a tidal encounter with another member of the group. In § 4 we investigate the effects of the resulting nonaxisymmetric velocity fields in the galactic disk on the generation of nonaxisymmetric fields. Further, we mention the possible effects of an azimuthal dependence of the turbulent parameters (η and α), directly attributable to the spiral structure, in § 5. Such a mechanism could be important if the disk turbulence was preferentially generated in the neighborhood of young hot stars in the spiral arms.

2. GALACTIC DYNAMO MODEL

We use the model of Paper I for the dependence of dynamo parameters on the distance (z) from the disk plane, namely,

$$\alpha = \alpha_0 z/(1 + \alpha_B \boldsymbol{B}^2)[1 + \alpha_1 - 2\alpha_1 e^{-(z/z_\alpha)^2}]$$
$$= \alpha_0 f(z)/(1 + \alpha_B \boldsymbol{B}^2) , \quad (1)$$

$$\eta = \eta_0[1 - \eta_1 e^{-(z/z_\eta)^2}] , \quad (2)$$

where α_0 and η_0 are constants. The computations discussed here have $\eta_1 = 0.95$, $\alpha_1 = -1$, corresponding to an enhanced halo resistivity and an α-effect concentrated toward the disk region (see Paper I). We assume $z_\alpha = z_\eta$.

Our rotation curve is based on that of Rohlfs & Kreitschmann (1980), but we found the steep gradients associated with the peak at small radius difficult to handle, and so used the broken curve shown in Figure 1. This generally resembles a Brandt type curve such as was used in Paper I.

We integrate the standard mean field dynamo equation

$$\partial \boldsymbol{B}/\partial t = \nabla \times (\boldsymbol{u} \times \boldsymbol{B} + \alpha \boldsymbol{B} - \eta \nabla \times \boldsymbol{B}) , \quad (3)$$

using a modification of the code described in Moss, Tuominen, & Brandenburg (1991b). Time is measured in units of the global diffusion time, R^2/η_0, and distance in units of R. We adopt a halo resistivity, $\eta_0 = 5 \times 10^{27}$ cm^2 s^{-1} and take $R = 15$ kpc. Our unit of time is thus 1.3×10^{10} yr and the unit velocity is $\eta_0/R \approx 10$ km s^{-1}. With prescribed rotation curve and η_0, the free dynamo parameter is

$$C_\alpha = \alpha_0 R/\eta_0 . \quad (4)$$

Putting $\alpha_B = 1$ in equation (1), the unit of $\boldsymbol{B}$ is $(\mu_0 \rho_0)^{1/2}\eta_0/R$, where ρ_0 is a typical value for the gas density in the disk, and we have assumed that the dynamical feedback is on the turbulent gas motions. In Paper I estimates for α in the range 10^5–10^6 cm s^{-1} are made: we here consider the magnitude of α to be a free parameter of this order of magnitude. The model used in § 5 is somewhat different. It should be emphasised now that the actual values of these parameters are quite uncertain, and so our computations can only demonstrate possible behaviors. Note that the magnitude of C_α may be a slightly misleading parameter, as the effective α-effect is modulated by the factor $f(z)$ (eq. [1]), even in the linear case with $\alpha_B = 0$.

Recent observations (Reynolds 1989; Cordes et al. 1991) suggest the presence of a relatively thick layer of neutral and ionized gas in the Milky Way, extending to a distance of order 1, ..., 1.5 kpc from the disk plane. A similar thick ionized disk has also been reported in NGC 891 (Rand, Kulkarni, & Hester 1990; Dettmar 1990). In the context of our model, these observations would suggest $z_\alpha = z_\eta \approx 0.1$. Although it may still be debatable whether such a thick disk is present in M81, the precise disk thickness is not of crucial importance for our idealized model, inasmuch as we try to indicate important mechanisms rather than to produce a definitive model. Our basically spherical dynamo code with its uniform distribution of grid points over r and θ is relatively inefficient in disk geometry, as many of the grid points are placed in the halo, where the gradients in the field structure are often smaller than in the disk. A more efficient version could allow a nonuniform distribution of grid points in meridional planes. We are thus limited to $z_\alpha = z_\eta \geq 0.2$, which is rather larger than required for a realistic galaxy model: this limitation should be kept clearly in mind. Thus, with these standard parameters, the maximum value of $f(z)$ is 0.17, and a maximum value of α of 7 km s^{-1} corresponds to $C_\alpha = 40$.

Equation (3) is solved by explicit integration in time using a modal expansion in ϕ on an explicit (r, θ) grid (r, θ, ϕ are spherical polar coordinates). The results described below were obtained on a 51×101 grid, uniformly distributed over $0 \leq r \leq 1$, $0 \leq \theta \leq \pi$, respectively, and azimuthal modes $m = 0$, 1, 2, 3 were included. Experimentation with different resolutions suggested that this gave satisfactory accuracy.

As in earlier papers (Rädler et al. 1990; Moss et al. 1991b), we define global parameters P and M to describe the field geometry, with $P = [E^{(S)} - E^{(A)}]/E_{\rm tot}$, $M = 1 - E(m = 0)/E_{\rm tot}$. $E^{(S)}$, $E^{(A)}$, $E_{\rm tot}$ are, respectively, the energies in the parts of the field symmetric and antisymmetric with respect to the disk plane and the total energy, and $E(m = 0)$ is the energy of the axisymmetric field.

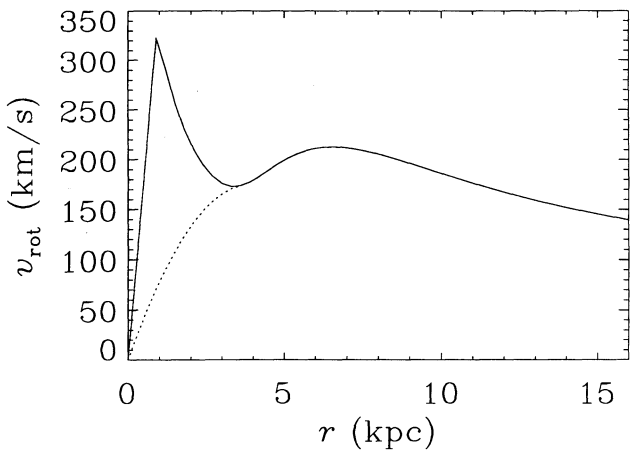

FIG. 1.—The Rohlfs & Kreitschmann rotation curve to 15 kpc (*solid curve*) and the rotation curve used (*dashed curve*).

3. RESULTS FROM THE STANDARD DYNAMO MODEL

Most of the calculations start with a seed field that contains large-scale structure with azimuthal dependence $m = 0$ and $m = 1$. The total initial energy is $E(0)$ and the corresponding ratio of nonaxisymmetric to axisymmetric energy is $q = M(0)[1 - M(0)]^{-1}$. The overall pattern of results can be illustrated by reference to Figure 2, which describes a computation with parameters $\alpha_1 = -1$, $\eta_1 = 0.95$, $E(0) = 10^{-12}$, $q = 10^4$, $C_\alpha = 40$. With this substantially supercritical value for C_α the growth rates of the $m = 1$ and $m = 0$ modes do not differ

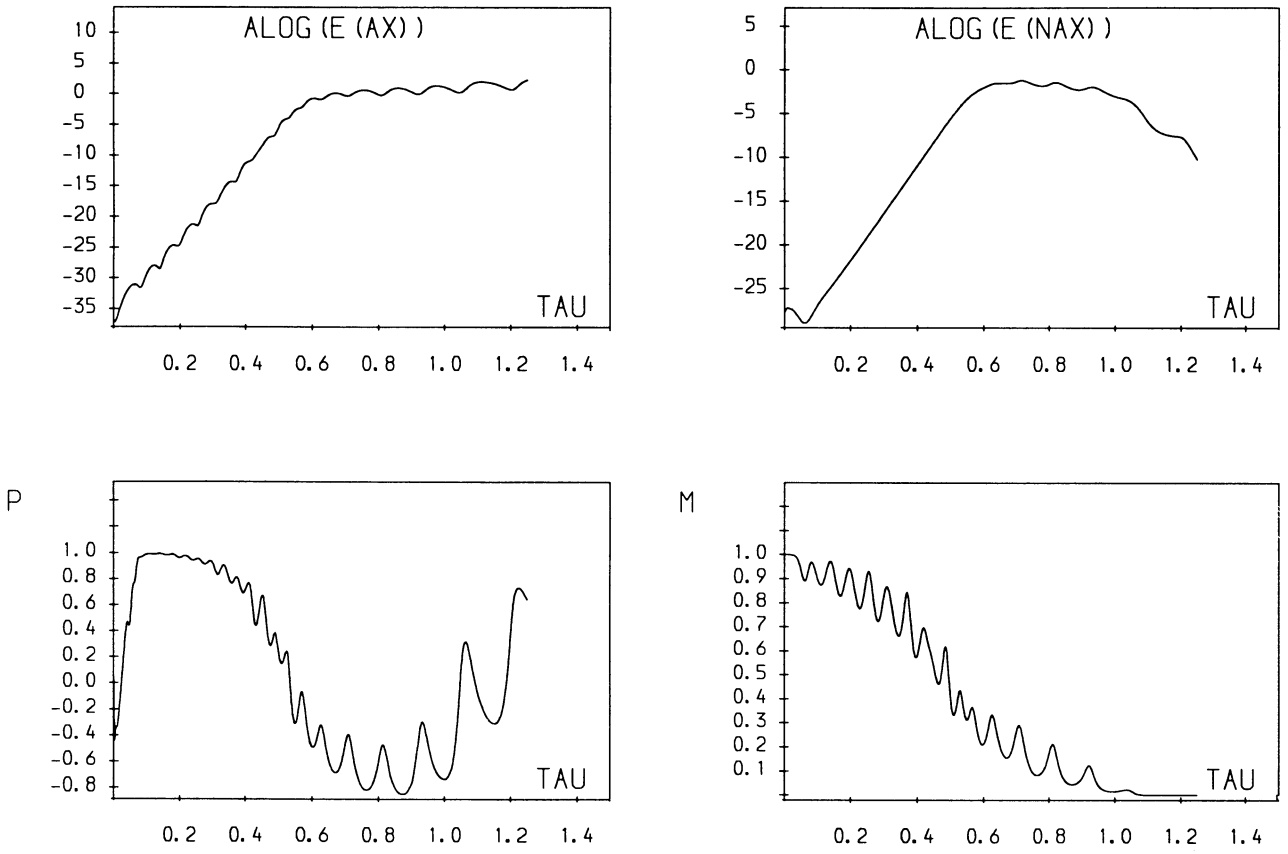

FIG. 2.—Results from computation with $C_\alpha = 40$, $\alpha_1 = -1$, $\eta_1 = 0.95$, $E(0) = 10^{-12}$, $q = 10^4$. From left to right, top to bottom: log $E(m = 0)$, log $E(m > 0)$, P, M.

very greatly, and M stays comparable to unity during the linear growth phase. After saturation is reached, the stable axisymmetric mode dominates ($P \rightarrow +1$ eventually in all these models), and M decreases to zero. There is an interval after $t = 0.6$ when the dynamo is saturated and M is significantly different from zero. The energy is modes with $m > 1$ is typically two or three orders of magnitude less than that in $m = 1$.

When q is larger/smaller, saturation is reached with a larger/smaller M value, and the decline of M to zero is delayed/accelerated. Similarily, when $E(0)$ is smaller/larger the time to saturation and subsequent decay of the nonaxisymmetric field component is longer/shorter. When C_α is smaller, growth rates are slower and, in general, the above phenomena occur at relatively later times. Figure 3 shows results from a computation with $C_\alpha = 30$, the other parameters unchanged from those of Figure 2. Here saturation occurs after about one diffusion time, and the value of M is then between 0.2 and 0.3. Note that in all cases the solutions were oscillatory, with typical periods of about 0.1 to 0.2 diffusion times. With larger values of z_α and z_η, the nonaxisymmetric fields are markedly less persistent.

The last panel of Figure 3 shows the evolution of the system in the $M-P$ plane. In this plane axisymmetric A0 and S0 fields are located in the lower left and upper left corners, respectively, whereas purely nonaxisymmetric A1 and S1 modes lie respectively in the lower and upper corners on the right hand side. Note that, after a short transient phase, the solution evolves in this diagram from the upper right corner (S1) toward the lower left corner (A0). Before reaching the A0 corner the solution turns toward the S0 corner, the location of the final stable solution. This indicates that there is not a direct transition from a S1 to a S0 solution, but that the system must pass through an intermediate mixed parity state (near to A0 to the $M-P$ plane). This phenomenon occurs even if the initial field has only a small $m > 0$ component. A similar "induced transition" phenomenon, but now from S0 to A0 via S1, was studied by Krämer (1989) and Rädler et al. (1990) in the context of spherical dynamos.

In Figure 4 we show a three-dimensional plot of field vectors where the field strength exceeds a certain threshold value. Note that in the inner parts there is clearly an axisymmetric field structure and that nonaxisymmetric contributions are only seen in the outer parts of the galaxy; see Figure 5. In addition, we show in Figure 6 field vectors parallel to the disk plane for $t = 1.0$.

We also performed some calculations with an initial field consisting of random $m = 0$ and $m = 1$ structure, with a typical length scale of 1 kpc. Results were qualitatively similar to those described above.

If α_1 is reduced in magnitude, to $\alpha_1 = -0.5$ or 0 say, then there is dynamo action throughout the halo region and the growth of nonaxisymmetric fields is strongly inhibited (in accordance with the usual arguments; see, e.g., Ruzmaikin et al. 1988; Moss & Brandenburg 1992). The stable field configuration is then of A0 type. When η_1 is decreased, the nonaxisymmetric field generation is again strongly inhibited and $M \rightarrow 0$ very rapdily for $\eta_1 < 0.8$.

4. EFFECTS OF NONAXISYMMETRIC VELOCITIES

Since M81 is a member of a group of galaxies, gravitational interactions with its neighbors have probably influenced its present appearance. There is a long tail of H I gas stretching from M81 to NGC 3077, another member of the group (van der Hulst 1979), and it seems likely that the latter galaxy passed close to M81 not long ago. Thomasson & Donner (1992) have investigated the hypothesis that the spiral structure of M81 has been caused by a recent interaction with NGC 3077 as it moves in a prograde orbit in a plane coinciding with the disk plane of M81. They followed the interaction of a point mass representing NGC 3077 with an N-body model of M81. The calculation was two-dimensional. About 430 Myr after the closest approach, the observed morphology and the relative positions and radial velocities of M81 and NGC 3077 were well represented by the model.

The resulting velocity field contains strong nonaxisymmetric components u_r, u_ϕ. These will interact with a purely axisymmetric magnetic field to generate nonaxisymmetric field components, even in the absence of any dynamo action in the nonaxisymmetric parts of the dynamo equation (3). Plausibly

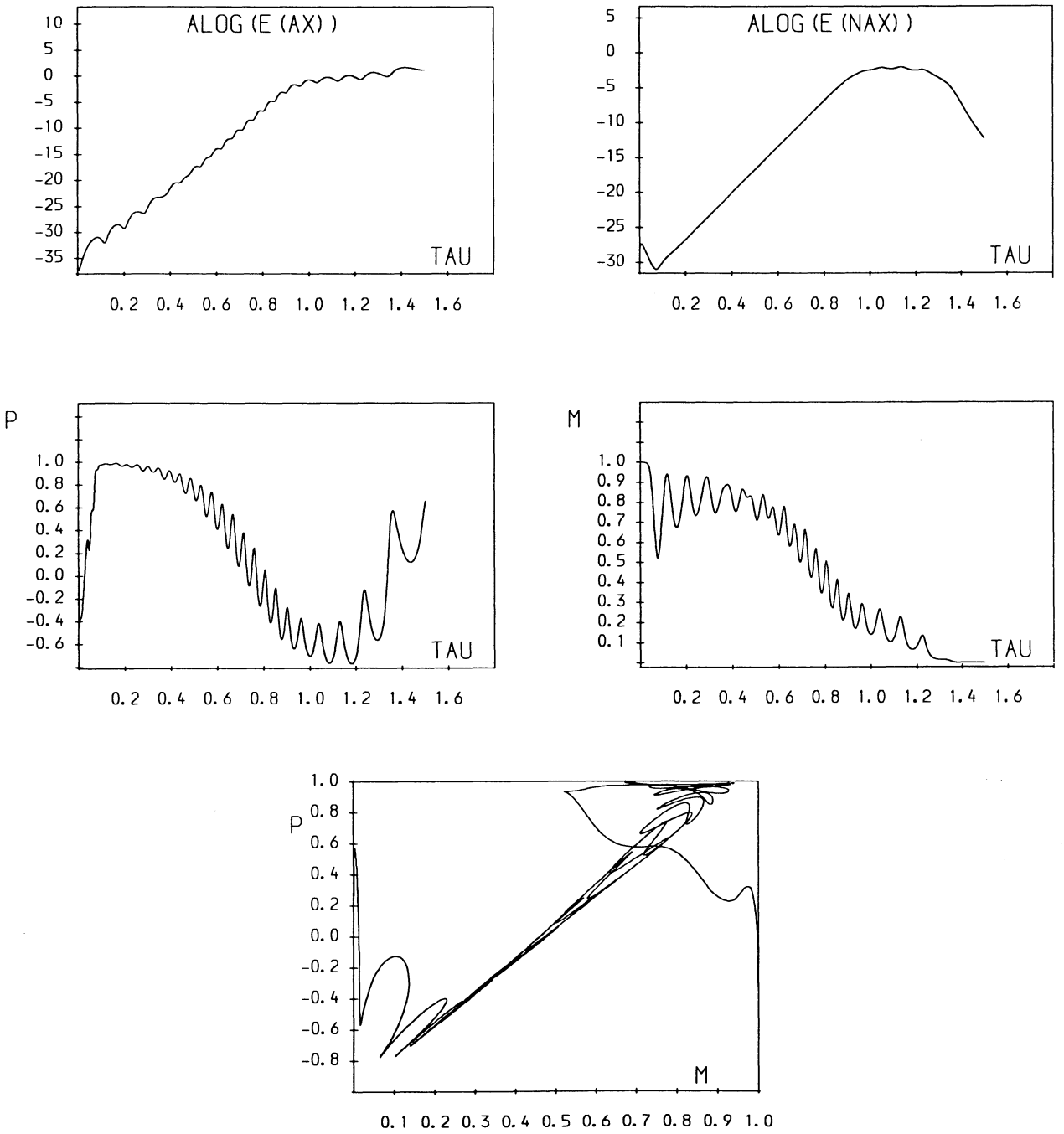

FIG. 3.—Results from computation with $C_\alpha = 30$, other parameters as Fig. 2. The bottom panel shows the variation of P with M during the calculation.

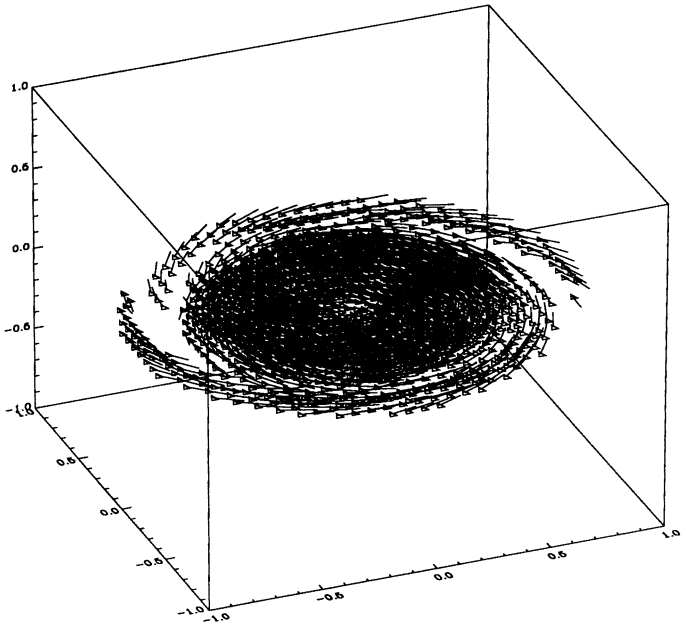

FIG. 4.—Three-dimensional plot of magnetic field vectors, where the field strength is larger than 50% of the maximum value (=1.8 in dimensionless units), for the model shown in Fig. 3 at $t = 1$. Axes are labeled in units of R, from -1.0 to $+1.0$.

any dynamo generation of $m > 0$ field could also be enhanced. Thus we made the investigations described below, using the axisymmetric rotation curve described in § 2, and an approximation to the nonaxisymmetric part of the velocity field computed by Thomasson & Donner. This involves a small inconsistency, as Thomasson & Donner used an initial rotation curve (i.e. the $m = 0$ part of the azimuthal motion) similar to the one in Visser's (1980) exponential disk model, which differs slightly from our rotation curve (Fig. 1), but qualitative results should not be affected.

Since the dynamical time scale of the tidal encounter is short compared with the time scale for magnetic field evolution, the field evolution should be calculated self-consistently, using the time-dependent velocity field. Our intention here is just to attempt to obtain an order of magnitude estimate of the size of the effect. For this reason we have taken the velocity field corresponding to the present time from the simulation and imposed this is as a constant velocity in the calculations of the magnetic field. As the general pattern of the velocity field is not changing very rapidly, this should give a reasonable first estimate of the importance of this mechanism. The velocity field, as reconstructed from the modes $m = 0, 1, 2, 3$, is shown in the upper panel of Figure 7. The lower panel shows the nonaxisymmetric part of the velocity, reconstructed from modes $m = 1, 2, 3$. These velocities can be interpreted as values in the plane $z = 0$, and we extend them out of the disk plane in a fairly arbitrary manner, by writing

$$u_{rm}(r, \theta) = u_{rm}(r, \pi/2) \sin \theta \; ; \quad u_{\phi m}(r, \theta) = u_{\phi m}(r, \pi/2) \sin^2 \theta \, , \tag{5}$$

where u_{rm}, $u_{\phi m}$ are the parts of u_r, u_ϕ with sin/cos $m\phi$ dependence. The z-dependence of α and η is as defined in § 2, with $z_\alpha = z_\eta = 0.2$.

The $m = 1$ and $m = 2$ velocity components are of comparable strengths. This might, at first, seem somewhat surprising, since prograde tidal encounters are known to produce $m = 2$ spirals, while a retrograde encounter is needed to produce an $m = 1$ spiral (Kalnajs 1975; Athanassoula 1978; Thomasson et al. 1989). In our case, NGC 3077 passed close to M81, and the disturbances in M81 were therefore not entirely symmetric but had somewhat different strengths on the sides close to and opposite to NGC 3077. This leads to an $m = 1$ component in the velocity field, even if the dominant structure is a two-armed trailing spiral (as shown by observations; e.g., Considère & Athanassoula 1988).

4.1. *Models with No Nonaxisymmetric Dynamo Action*

In order to isolate the effects of the imposed nonaxisymmetric velocity field we first computed strictly axisymmetric α-quenched dynamo fields of S0 type. In these models, the nonaxisymmetric field components arise solely from the term $\boldsymbol{u} \times \boldsymbol{B}$ in equation (3). We considered successively models with uniform α, η (i.e., $\alpha_1 = \eta_1 = 0$); $\alpha_1 = -1$, $\eta_1 = 0$; $\alpha_1 = -1$, $\eta_1 = 0.95$. With slightly supercritical C_α values we typically obtained modest nonaxisymmetric field strengths, with M values in the approximate range of 0.05 to 0.10. The nonaxisymmetric energy was predominantly in the $m = 1$ field in

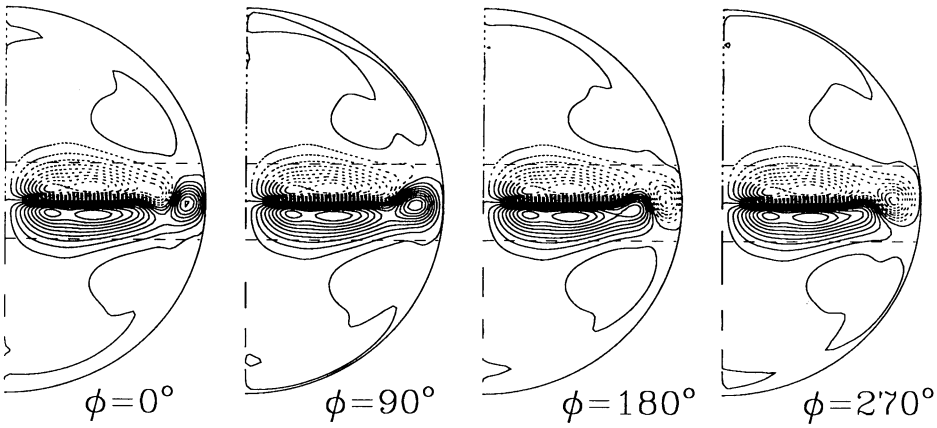

FIG. 5.—Contours of B_ϕ in four different meridional planes ϕ = const for the model shown in Figs. 3 and 4 at $t = 1$. Here broken contours indicate negative values, and the position of the disk plane, $|z| = z_\alpha = 0.2$, is indicated by dashed lines. Note that in the inner parts the field is predominantly antisymmetric about the disk plane, but symmetric in the outer parts.

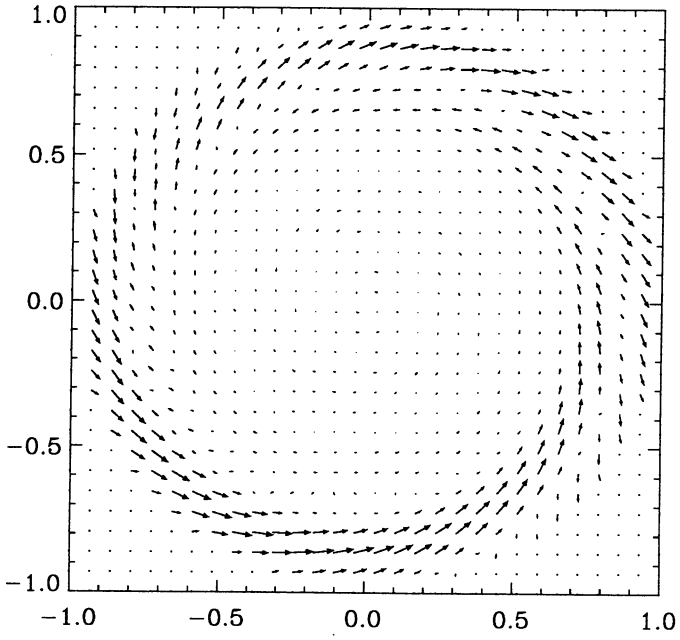

FIG. 6.—Magnetic field vectors in the equatorial plane for the model of Fig. 3 at $t = 1$. In the inner parts the field is rather weak in the plane $z = 0$, because it is almost exactly antisymmetric about the disk plane (see Fig. 5). It is, of course, stronger above and below this plane.

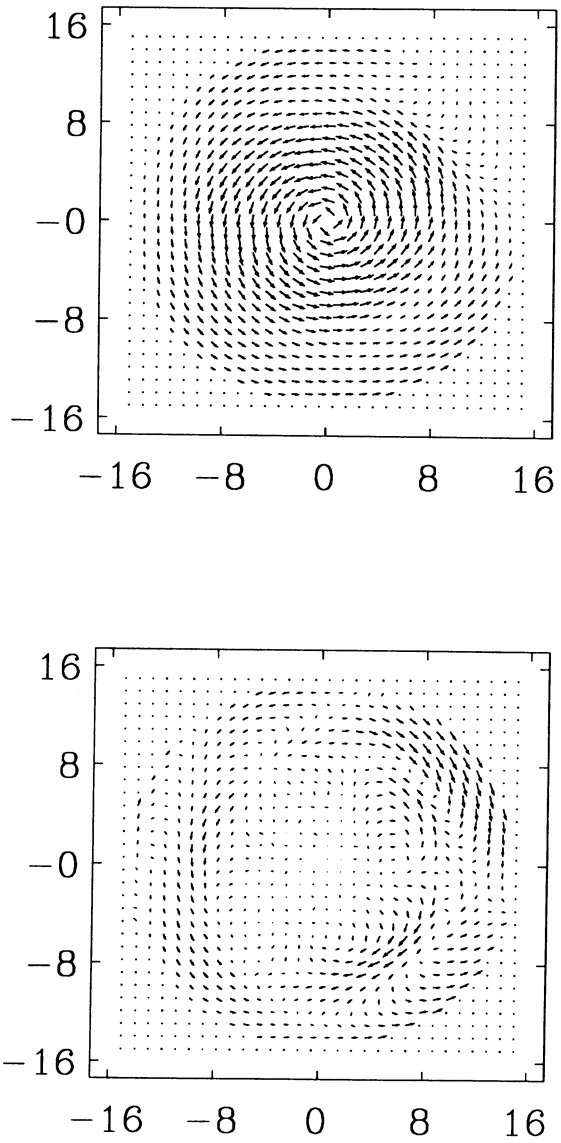

FIG. 7.—Velocity field vectors in the disk plane from Thomasson & Donner's simulations, as used in the model illustrated in Fig. 8. *Top panel*: all components included. *Bottom panel*: from $m = 1, 2, 3$ components only. Scale is in kiloparsecs

each case, and the field configurations did not vary strongly between the different models considered.

4.2. *Dynamo Model of Section 2*

We now took $\alpha_1 = -1$, $\eta_1 = 0.95$ in the full dynamo model described in § 2 and used in § 3, and included the interaction between the $m = 0$ magnetic field and the $m > 0$ velocities explicitly. In this case we neglected the interaction between the $m > 0$ fields and the $m > 0$ velocities: unless M is large this should be a reasonable approximation and should anyway allow us to assess the efficiency of enhancement of non-axisymmetric field generation by this mechanism. Plausibly, the inclusion of these neglected terms would delay the decline of M from its initial value of near unity. With $C_\alpha = 40$, $E(0) = 10^{-12}$, $q = 10^4$ [i.e. $M(0) = 0.9999$], we found that M was somewhat larger (see Fig. 8) than in the corresponding calculation of § 3 (Fig. 2), but that the difference is only really noticeable when the value of M given by Figure 2 had become small. The saturated regime now has M oscillating near a value of 0.1. The energy in $m > 1$ is $\sim 35\%$ of that in $m = 1$. With $C_\alpha = 30$, this figure drops to $\sim 25\%$.

In Figure 9 we show a three-dimensional plot of field vectors where the field strength exceeds a certain threshold value. Note that the magnetic field is on one side much stronger than on the other.

Note that even if the initial field were to have no $m = 0$ component (physically unrealistic), with this model the interaction between the $m > 0$ velocity and magnetic fields would generate a $m = 0$ magnetic field, and so the eventual configuration would contain strong axisymmetric contributions.

5. EFFECTS OF IMPOSED NONAXISYMMETRIC STRUCTURE

Moss, Brandenburg, & Tuominen (1991a) made a preliminary investigation of the effects of imposing a $m = 1$ dependence in $\alpha(r)$, and found that, in a simple spherical model, $m = 1$ modes were readily excited in an α^2-dynamo, but that differential rotation strongly inhibited these modes in an $\alpha^2\omega$ dynamo. These models were very idealized in that disk geometry and truly spiral (as opposed to simple non-axisymmetric "spokelike") effects were not studied. However, there is a more fundamental problem with explaining $m = 1$ field structure in galaxies by this sort of mechanism, in that in most galaxies spiral arms have a predominantly even m structure, in contrast to the predominantly $m = 1$ observed field in M81 (e.g., Krasheninnikova et al. 1990). (M51, in contrast, does have a predominantly $m = 1$ arm structure, but its magnetic field does not seem to have a simple classification in terms of one or two low-order azimuthal modes.)

A possible solution to this problem is that, if there is a slight asymmetry between the spiral arms, a more appropriate repre-

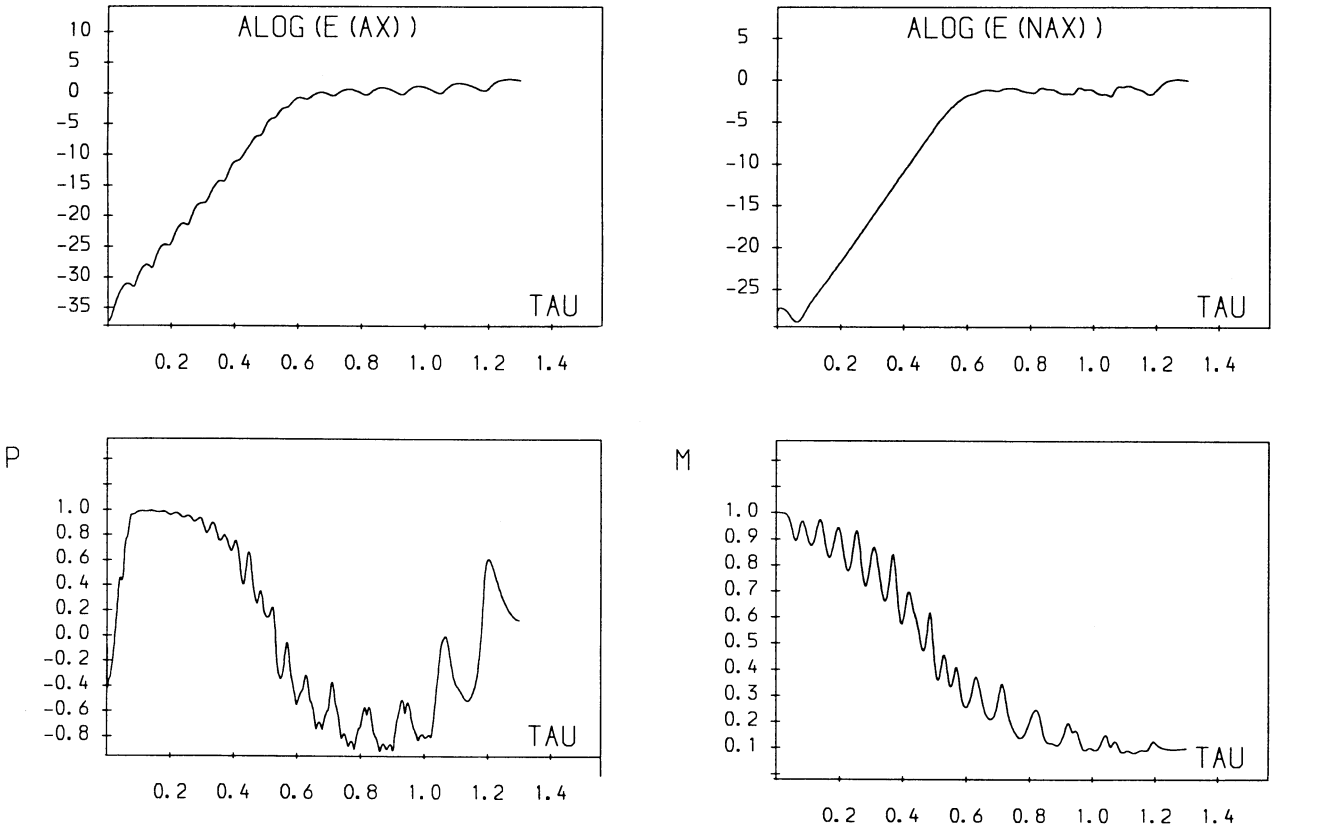

FIG. 8.—Calculation with parameters as for Fig. 2, but with addition of nonaxisymmetric velocities

sentation might be, for example

$$\alpha = \tilde{\alpha}_0(r, \theta)(1 + a_1 \cos \phi + a_2 \cos 2\phi) , \quad (6)$$

with $|a_1| \ll |a_2|$. The interaction of the cos 2ϕ term in (6) with a $m = 1$ magnetic field generated by the cos ϕ term in equation (3) (the $m = 1$ field being generated by the cos ϕ term in eq. [6]) will generate $m = 1$ and $m = 3$ components of equal magnitude, but any $m > 1$ field will decay much more readily than the $m = 1$.

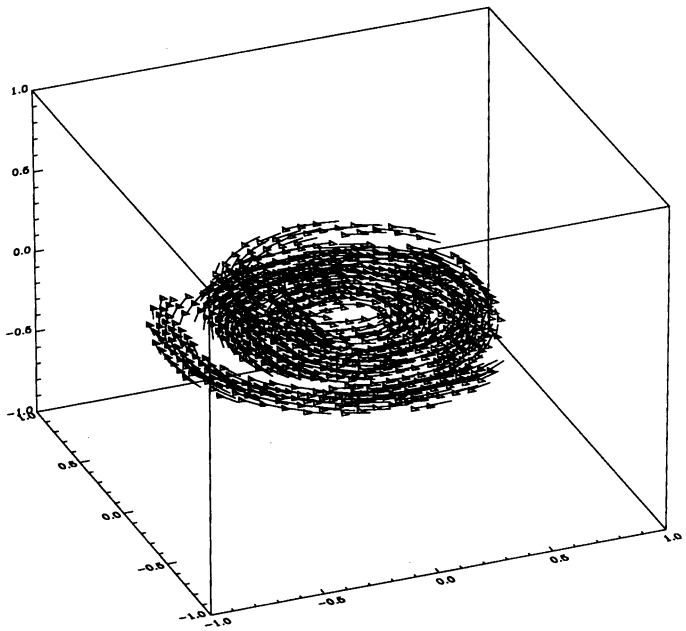

FIG. 9.—Three-dimensional plot of field vectors, where the field strength is larger than 50% of the maximum value (= 5.3 in dimensionless units), for the model of Fig. 8 at $t = 1$. Axes are labelled in units of R, from −1.0 to +1.0.

Accordingly the code used in Moss et al. (1991a) was modified to include an α-effect of the form given by equation (6), and also to include a resistivity of the form

$$\eta = \eta_0(1 + \eta_2 \sin \theta \cos 2\phi) , \quad (7)$$

with η_0 and η_2 constants. The sin θ factor is needed to make the ϕ-dependent part of η vanish on the axis, otherwise the solution is not well behaved there. (Strictly a sin θ factor should, for consistency, be present in the nonaxisymmetric part of α in eq. [6], but in practice its omission does not seem to affect adversely the solution. We note also that the ϕ-dependence of η gives a contribution to the nonaxisymmetric poloidal equation proportional to the nonaxisymmetric toroidal field, allowing in principle a completion of the dynamo cycle "poloidal → toroidal → poloidal" without recourse to an α-effect. However, this term does not seem able to replace the α-effect to drive a dynamo. See also Donner & Brandenburg 1990a.)

We first looked at linear modes of α^2 dynamos in a sphere with $\eta_2 = 0$, $0.2 \leq a_2 \leq 1$, and $0.05 \leq a_1 \leq 0.2$. Our technique was simply to integrate equation (3) until exponential behavior (steady or oscillatory) was found, with the different m-modes locked (see Moss et al. 1991a). With, for example, $a_1 = 0.1$, $a_2 = 0.5$, $\eta_2 = 0$, we found a solution with $M \approx 0.8$, and the majority of the nonaxisymmetric energy in the $m = 1$ part of the field. Putting $\eta_2 = a_2$ converted a steady solution into one that oscillated between about $M = 0.3$ and $M = 0.8$, on a time

TABLE 1

SUMMARY OF CALCULATIONS WITH NONAXISYMMETRIC α-EFFECT[a]

h	C_α	M	λ
0.30	200	0.08	0.0
0.30	250	0.12	4.8
0.25	400	0.20	6.6
0.20	600	0.24	3.2

[a] NOTE.—$a_1 = 0.05$, $a_2 = 0.5$, $\eta_2 = 0.5$, $C_\omega = 400$. $\lambda = \frac{1}{2} d \ln E/dt$ is the growth rate.

scale comparable to a diffusion time. We then investigated "galactic" models with the Brandt type rotation curve used in Paper I and an α coefficient that was confined to the disk $|z| < h$ and was zero at $z = 0$ and in $|z| > h$:

$$\tilde{\alpha}_0 = \alpha_0 p^2(3 - 2p)z = \alpha_0 g(z)z \,, \tag{8}$$

where $p = (h - |z|)/h$ for $0 < |z| < h$ and $p = 0$ for $|z| > h$. (Thus both the rotation curve and the expression for α in this model are somewhat different to those used in the preceding sections.) With the spatial resolution available, we found it impossible to get reliable results with a disk thickness h much less than about $h = 0.25$. With $a_1 = 0.05$ and $a_2 = 0.50$, we found linear solutions with $M \approx 0.10, \ldots, 0.25$, with some evidence that the M values attainable increase as h decreases. The energy in the $m > 1$ part of the field was of order 1% of that in the part with $m = 1$. M also appears to increase as C_α becomes more supercritical for a given rotation law. The range of supercritical C_α for which we felt our code to be reliable was, however, quite small for small values for h. We were not able to produce unambiguous evidence for solutions with values of M near to unity. Some illustrative values of growth rates are given in Table 1. We note that these values are rather smaller than values found for the models discussed in previous sections, which generally have $\frac{1}{2} d \ln E/dt$ of order 15 in the linear regime for moderately supercritical C_α. The difference is probably attributable to the different functional forms for α and to differing supercriticality of the model. Once again note that the effective value of C_α is reduced by the factor $g(z)$ in expression (8).

6. DISCUSSION

A major uncertainty in evaluating the significance of our computations is the unknown nature of the seed field. This question is discussed in detail in Rees (1987) and Ruzmaikin et al. (1988). If the seed is present in the intergalactic medium, then its magnitude is quite uncertain. Current intergalactic field strengths seem to be less than $\sim 10^{-11}$ G (e.g., Vallée 1983) and potential seed fields may have been less than $\sim 10^{-18}$ G (e.g., Rees 1987). But see also Coles (1992). Any such a seed might have been compressed to larger magnitude during the initial collapse of the protogalactic material. Seed fields of this nature might be expected to be of galactic scale. Alternatively, if the seed originated inside the galaxy after the initial collapse, then the seed field scale would be smaller and strength possibly larger (e.g., Ruzmaikin et al. 1988). M81 may be a special case because of its encounter with NGC 3077, which conceivably could have "reset the clock," and imposed nonaxisymmetric structure at a relatively late stage, in addition to any ongoing effects from persisting nonaxisymmetric velocities, such as discussed in § 4.

Our rotation curve omits the strong gradients at small radii suggested by Rohlfs & Kreitschmann (1980). This may not be too important, as strong differential rotation tends to favor axisymmetric field generation, and the inner disk is already dominated by axisymmetric field.

The calculations reported in § 3 suggest that a small degree of nonaxisymmetric structure might survive for times of order 10^{10} yr in a moderately flattened disk geometry, with fields in approximate equipartition with the energy of the turbulent gas motions. For our standard parameters we find only $M = O(0.1)$. It is difficult to compare this value with observations of M81, although it is probably rather low. In our models the nonaxisymmetric structure is concentrated to the outer regions of the disk—see Figures 4 and 6—which may make it somewhat more conspicuous than suggested by the value of M. This effect is naturally explained by the relatively small differential rotation in the outer part of the disk.

An alternative to a nonaxisymmetric seed field is that the observed field structure in M81 is due, in part at least, to the distortion of an axisymmetric field by nonaxisymmetric velocities. In § 4 we presented calculations including this effect using an approximation to the velocities in the tidal model of Thomasson & Donner (1992). Although a time-dependent velocity field should be use to allow a proper comparison with observations, our results do appear to have the correct qualitative behavior.

If the tidal model is correct, it would also explain why only M81 displays evidence for BSS field structure. The only other interacting systems with well-observed field structure is M51. Recently, earlier claims for the presence of a BSS field in M51 have been put into doubt (M. Krause, private communication). Coincidentally, Engström & Athanassoula (1992) have recently proposed a new dynamical model for the M51/NGC 5195 system, in which the interaction took place much earlier, and at a greater separation, than has hitherto been assumed. Because of the large distance of closest approach, the $m = 1$ component of the tidal perturbation would be greatly reduced in the inner disk.

In deducing field structure from observations, polarization and rotation measure RM are important quantities. It is interesting to see how our computed field structures might appear to an observer. For example, note that in Figure 6 the axisymmetric field component is antisymmetric with respect to the disk plane (A0), whereas the nonaxisymmetric component is symmetric (S1). Thus, on measuring the polarization, there will be some cancellation of the axisymmetric component, possibly leaving an apparent dominance of the contribution from the S1 part of the field. Such a phenomenon might have important consequences for the interpretation of observations.

In Figure 10 we show the rotation measure, RM, calculated for the model of Figure 3 at time $t = 0.75$ and $t = 1.0$. RM was evaluated as a function of the position angle ψ using the method described in Donner & Brandenburg (1990b) using the same parameters for the electron distribution as in Brandenburg et al. (1992). Note that only in the outer parts ($r/R = 0.8$) is there a doubly peaked dependence of RM on ψ, manifesting the nonaxisymmetric structure there. In the inner parts ($r/R = 0.4$) the RM curve is singly peaked, whereas for intermediate radii (say $r/R = 0.6$) the variation with ψ is more complicated. For comparison, we show in Figure 11 the variation of RM for the model described in § 4 at times $t = 0.75$ and

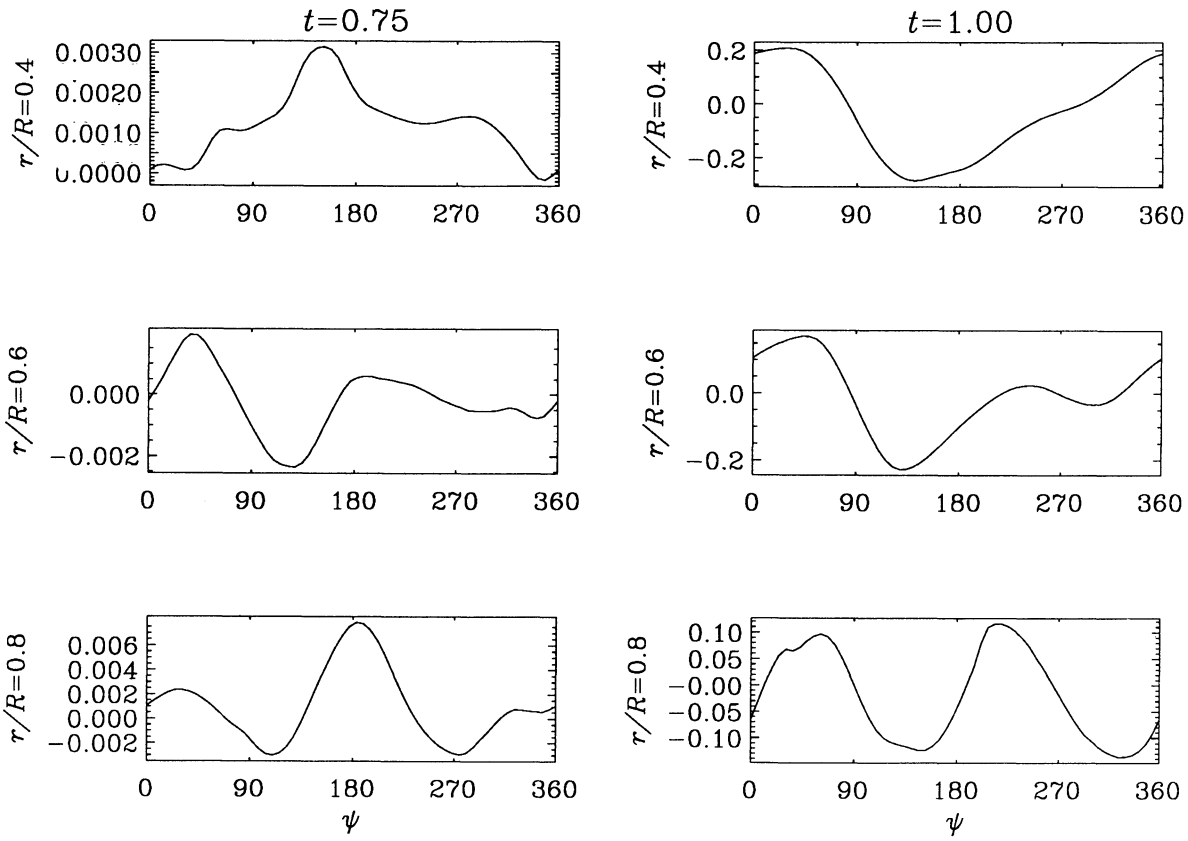

FIG. 10.—Dependence of the rotation measure on the position angle for the model of Fig. 3 at $t = 0.75$ and $t = 1.0$ at different radii and an inclination of 50°. Note the doubly peaked variation for $r/R = 0.8$.

$t = 1.0$. A doubly peaked variation with position angle is only seen in the outer parts at $t = 1.0$. This behavior is less clearly defined than in the case of our standard model (see Fig. 10). These simple calculations, like those in Paper I, show that interpretation of observations in terms of field structure is quite model dependent (see also Donner & Brandenburg 1990b; Elstner, Meinel, & Beck 1992).

We note that we have not produced a good model for M81, in that our field structure does not resemble closely the observed field. In particular, RMs suggest the presence of nonaxisymmetric field structure at radii less than 9 kpc (Krause et al. 1989), whereas in our models it only appears strongly at significantly larger radii. We *do* feel that we have demonstrated the potential importance of several mechanisms for the generation of the BSS structure of M81. Our model is inevitably considerably simplified—most notably in taking a relatively large disk thickness parameter of 0.2. A thinner disk (i.e., smaller z_α, z_η values) makes the growth rates of $m = 0$ and $m = 1$ modes more nearly equal; cf. Table 1 of Moss & Brandenburg (1992). (Note that the disk thickness z_0 defined there is not the same as z_α; a given value of z_0 correspondings approximately to a rather smaller value of z_α. Also their model did not include a z-dependent η.) We speculate that if calculations analogous to those of § 3 were performed with $z_\alpha = z_\eta = 0.1$ or less, then M would be enhanced at times of $O(10^{10})$ yr, with the probable consequence that the nonaxisymmetric structure would extend to smaller radii. The calculations of § 5 strongly suggest that azimuthal structure in the turbulence may also promote a significant amount of nonaxisymmetric field structure and, although we have not made a fully self-consistent study, including simultaneously a ϕ-dependence in α and η in the model of §§ 3 and 4, we can expect that such a model would further favor the generation of BSS structure. Finally, it should be noted that the α effect in galaxies is likely to be highly anisotropic (Rüdiger 1990), and that this can also favor nonaxisymmetric field generation (Meinel et al. 1990).

We note that our ideas do not result in predominant $m > 0$ fields, but that the lastest observational evidence (Sokoloff, Shukurov, & Krause 1992) does suggest the presence of a significant $m = 0$ component in M81. Also we would in general expect a small $m = 2$ contribution—again this may be observed.

As yet our models are not sufficiently sophisticated for observations to distinguish between the different field generation mechanisms. In particular, as noted above, we have only treated the effects of larger-scale azimuthal structure in the turbulence in a very idealized manner. Indeed, there is no reason why any one of these mechanisms should act alone in a real galaxy.

Recently there has been a report of BSS structure in a remote galaxy (Kronberg, Perry, & Zukowski 1992), with a redshift $z \approx 0.395$. Given the history of controversy of reported incidence of BSS fields in nearby galaxies, it will be interesting to see if this finding is confirmed. It has been suggested that the presence of equipartition strength magnetic fields of any large scale geometry in such a young galaxy poses a problem for dynamo theory. Our calculations indicate that this suggestion is not necessarily valid: there is considerable uncertainty in

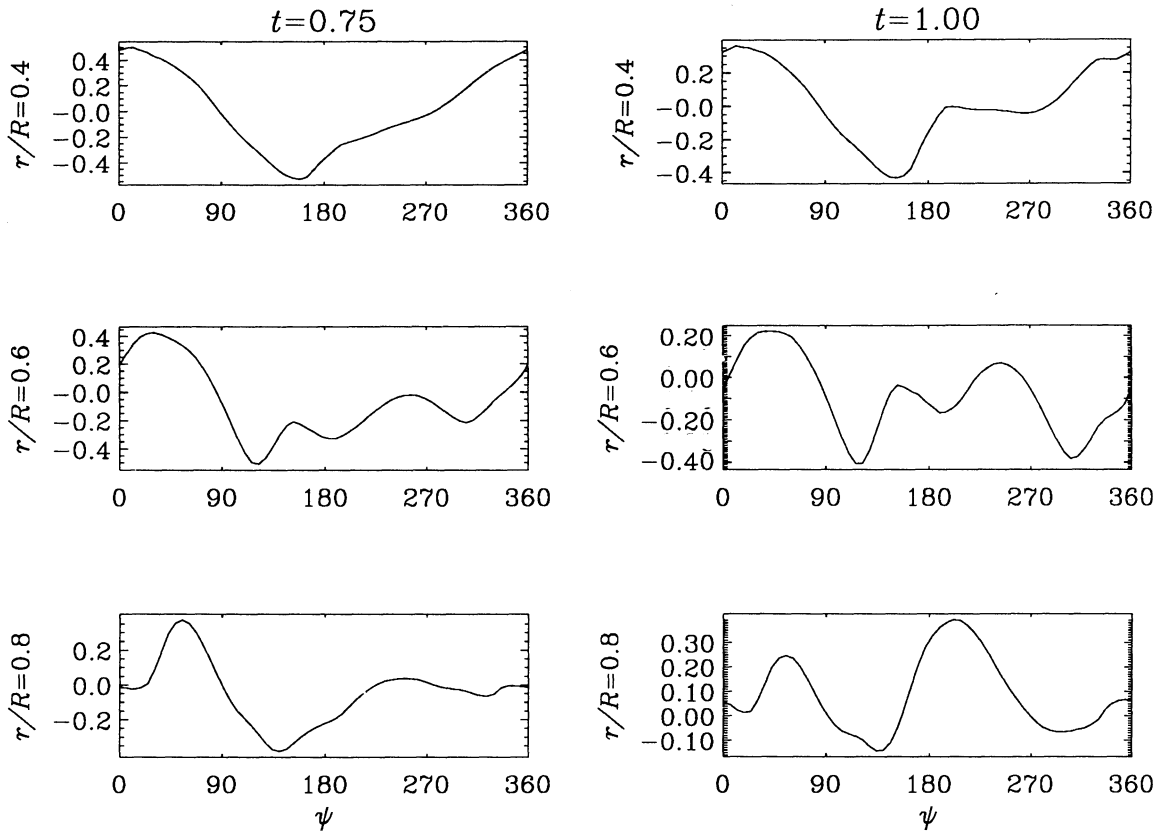

FIG. 11.—The same as Fig. 10, but for the model of Fig. 8

seed field strength, and growth rates depend very sensitively on C_α. For example, in even our standard model (Fig. 2) saturation occurs after $t \approx 0.6$, that is $\sim 8 \times 10^9$ yr, with $C_\alpha = 40$. If C_α were to be doubled to 80, the growth rates would increase by a factor of ~ 2.5–3, and for the same seed field equipartition would then occur after $\sim 3 \times 10^9$ yr. It is also quite arguable that younger galaxies might have more young, hot stars, OB associations, etc., resulting in stronger turbulence and a larger C_α value.

It is certainly true that in our standard model of § 3, at least, we have to choose parameters fairly carefully in order to produce long-lived BSS type structure although, in principle at least, in the tidal interaction model some uncertainties could be reduced by improved modeling. In particular, in the absence of other effects, the seed field needs to have predominant $m > 0$ structure (e.g., a uniform or dipolar field approximately perpendicular to the disk axis, if of galactic scale), although this requirement might be somewhat relaxed with a thinner disk. (Other neglected effects may also encourage nonaxisymmetric field generation, see the above discussion.) For our particular problem (M81), this is not necessarily a drawback: observations now show this to be the only nearby galaxy with strong $m > 0$ structure. Of course, small number statistics are notorious, and we await a larger sample with interest.

We thank Anvar Shukurov and Dmitry Sokoloff for their thought-provoking comments.

REFERENCES

Athanassoula, E. 1978, A&A, 69, 395
Beck, R. 1990, Geophys. Astrophys. Fluid Dyn., 50, 3
Brandenburg, A., Donner, K. J., Moss, D., Shukurov, A., Sokoloff, D. D., & Tuominen, I. 1992, A&A, 259, 453 (Paper I).
Brandenburg, A., Krause, F., Meinel, R., Moss, D., & Tuominen, I. 1989, A&A, 213, 411
Coles, P. 1992, Comments Astrophys., 16, 45
Considère, S., & Athanassoula, E. 1988, A&AS, 76, 365
Cordes, J. M., Weisberg, J. M., Frail, D. A., Spangler, S. R., & Ryan, M. 1991, Nature, 354, 121
Dettmar, R.-J. 1990, A&A, 232, L15
Donner, K. J., & Brandenburg, A. 1990a, Geophys. Astrophys. Fluid Dyn., 50, 121
———. 1990b, A&A, 240, 289
Elstner, D., Meinel, R., & Beck, R. 1992, A&AS, 94, 587
Elstner, D., Meinel, R., & Rüdiger, G. 1990, Geophys. Astrophys. Fluid Dyn., 50, 85
Engström, S., & Athanassoula, E. 1992, preprint
Kalnajs, A. J. 1975, in La Dynamique des Galaxies Spirales, ed. L. Weliachew (Paris: Centre National de la Recherche Scientifique), 103
Krämer, A. 1989, GAMMA 48, Dipl. thesis, Tech. Univ. Braunschweig
Krasheninnikova, Yu. S., Sokoloff, D. D., Ruzmaikin, A. A., & Shukurov, A. 1990, Geophys. Astrophys. Fluid Dyn., 50, 131
Krause, M., Beck, R., & Hummel, E. 1989, A&A, 217, 17
Kronberg, P. P., Perry, J. J., & Zukowski, E. L. H. 1992, ApJ, 387, 528
Meinel, R., Elstner, D., & Rüdiger, G. 1990, A&A, 236, L33
Moss, D., & Brandenburg, A. 1992, A&A, 256, 371
Moss, D., Brandenburg, A., & Tuominen, I. 1991a, A&A, 247, 576
Moss, D., & Tuominen, I. 1990, Geophys. Astrophys. Fluid Dyn., 50, 133
Moss, D., Tuominen, I., & Brandenburg, A. 1991b, A&A, 245, 129
Perry, J. J., Watson, A. M., & Kronberg, P. P. 1992, preprint
Rädler, K.-H., Wiedemann, E., Brandenburg, A., Meinel, R., & Tuominen, I. 1990, A&A, 239, 413
Rand, R. J., Kulkarni, S. R., & Hester, J. J. 1990, ApJ, 352, L1
Rees, M. J. 1987, QJRAS, 28, 197
Reynolds, R. J. 1989, ApJ, 339, L29

Rohlfs, K., & Kreitschmann, J. 1980, A&A, 87, 175
Rüdiger, G. 1990, Geophys. Astrophys. Fluid Dyn., 50, 53
Ruzmaikin, A. A., Shukurov, A. M., & Sokoloff, D. D. 1988, The Magnetic Fields of Galaxies (Dordrecht: Kluwer)
Sofue, Y., Fujimoto, M., & Wielebinski, R. 1986, ARA&A, 24, 469
Sokoloff, D., Shukurov, A., & Krause, M. 1992, A&A, in press, 264, 396
Stepinski, T. F., & Levy, E. H. 1988, ApJ, 331, 416
Thomasson, M., & Donner, K. J. 1992, A&A, submitted
Thomasson, M., Donner, K. J., Sundelius, B., Byrd, G. G., Huang, T.-Y., & Valtonen, M. J. 1989, A&A, 211, 25
Vallée, J. P. 1983, Astrophys. Lett., 23, 85
van der Hulst, J. M. 1979, A&A, 75, 97
Visser, H. C. D. 1980, A&A, 88, 149